NASA TN D-1431

TECHNICAL NOTE

D-1431

AN EXPERIMENTAL INVESTIGATION OF THE IMPACT RESISTANCE OF DOUBLE-SHEET STRUCTURES AT VELOCITIES TO 24,000 FEET PER SECOND

By C. Robert Nysmith and James L. Summers

Ames Research Center
Moffett Field, Calif.

NATIONAL AERONAUTICS AND SPACE ADMINISTRATION
WASHINGTON
October 1962

NATIONAL AERONAUTICS AND SPACE ADMINISTRATION

TECHNICAL NOTE D-1431

AN EXPERIMENTAL INVESTIGATION OF THE IMPACT RESISTANCE OF DOUBLE-SHEET STRUCTURES AT VELOCITIES TO 24,000 FEET PER SECOND

By C. Robert Nysmith and James L. Summers

SUMMARY

Small pyrex glass spheres, representative of stoney meteoroids, were fired into double-sheet structures at velocities to 24,000 feet per second to determine the effects of a number of target variables upon penetration resistance. It was observed that the impacts could be classified into various categories as a function of the impact velocity: a low-speed impact region, a transition region, and a high-speed impact region. The regions are discussed and illustrated by individual frames from high-speed motion pictures of the impact process. It is noted that results obtained in one region of impact are not applicable to the others.

The effects of combined sheet thickness and sheet spacing upon penetration resistance were investigated for the low-speed and the high-speed regions of impact. It was determined that the required total sheet thickness varies with the first power of the velocity in the low-speed impact region and appears to vary with the 2/3 power of the velocity in the high-speed impact region. It was also observed that increases in spacing between sheets resulted in only slight increases in penetration resistance at low speeds. However, in the transition and high-speed impact regions, spacing became very much more effective in controlling the performance of the structure.

It was concluded that structures having front sheets with equal mass per unit area and identical rear sheets have the same penetration resistance for several front-sheet materials. Also, for maximum penetration resistance per unit weight, the available structural weight should be concentrated in the rear sheet with the front sheet only thick enough to shatter the projectile completely.

A discussion and illustrations of oblique impact on double-sheet structures are also presented.

INTRODUCTION

A program of research directed toward determining the impact resistance of composite structures is at present being conducted in the Hypervelocity Ballistic Range of the Ames Research Center. The results of a preliminary portion of this investigation were reported in reference 1. In the reference report, the impact resistance of a limited number of simple double-sheet and four-sheet structures was determined at velocities to 11,000 feet per second. One purpose of the present report is to present double-sheet structure impact data at velocities to 24,000 feet per second and to show that composite target impact results obtained at low speeds are not applicable at high speeds. Another purpose of the present report is to determine the effects upon structural penetration resistance of such target variables as the combined sheet thickness, the sheet spacing, the distribution of weight between front and rear sheets, the front sheet material, and impact at oblique angles.

NOTATION

d diameter of spherical projectile, in.

D diameter of hole in first sheet, in.

h spacing between sheets, in.

t_1 thickness of first sheet, in.

t_2 thickness of second sheet, in.

t_T combined thickness of first and second sheet, $t_1 + t_2$, in.

V velocity of projectile at impact, ft/sec

EXPERIMENTAL PROCEDURE

The tests were conducted by firing small projectiles from a light-gas gun into double-sheet targets at velocities to 24,000 ft/sec.

The projectiles were small pyrex glass spheres with a density of 2.23 grams per cubic centimeter and varied in diameter from 1/16 inch to 3/16 inch. Glass was selected because it shatters upon impact and thus is considered to be representative of stoney meteoroids. The spheres were mounted in supporting sabots which guided them down the bore of the gun barrel and protected them from the damaging effects of the propellant gases. After launch, the sabots were separated from the models and deflected to prevent them from damaging the targets. Spark photographs

of the models were taken at numerous stations, and intervals of time and distance were measured. The velocity as well as the physical condition of the model in flight was determined from the above data. A detailed description of the experimental apparatus employed is provided in reference 1.

The targets were multiple-sheet structures consisting of two sheets of material placed one behind the other with a 0.016-inch-thick 2024-T3 aluminum alclad "witness" sheet 1/2 inch behind the test structure. The witness sheet is useful in assessing the damage to the basic structure. In all tests, the second sheet of the main structure was 2024-T3 aluminum alclad. After impact, the second sheet was subjected to a pressure difference of one atmosphere to detect the presence of any leaks. The specific gravity of the front sheet materials ranged from 1.2 to 8.5, and sheet spacing (distance between the first and second sheets) was varied from 1/2 inch to 1.5 inches.

In most tests, the targets were alined with the front face normal to the projectile trajectory. In one series of tests, however, the target was alined with the front face 45° to the projectile trajectory.

All targets tested in the above investigations were at a zero stress level and at room temperature when impact occurred. In reality, hull structures for space vehicles will probably be load-carrying members so that when they are impacted the damage will tend to be more severe. For reasons of simplicity, this factor is neglected in the investigations considered in this report.

RESULTS AND DISCUSSION

Regions of Impact and the Effects of Total Sheet Thickness and Sheet Spacing

Tests were conducted to determine the effects of combined thickness and sheet spacing upon structural resistance to penetration. All structures in this series of tests consisted of two sheets of 2024-T3 aluminum alclad placed one behind the other. The variables included the combined sheet thickness, the sheet spacing, and the impact velocity. When a particular sheet thickness combination was selected for investigation, an attempt was made to divide the combined thickness equally between the front and rear sheets. The penetration resistance of the structures was measured in terms of the structure's "ballistic limit." This term is defined here as the projectile velocity required to damage the rear sheet of a structure so that it will no longer hold a pressure difference of one atmosphere without leaks. This criterion thus takes into account the material spalled from the rear of the second sheet through the pressure differential test. On the other hand, it does not differentiate between failures due to individual particle craters and those resulting from cracks produced by the effective pressure pulse exerted by the cloud of

small particles striking the sheet. However, it was observed that when impact velocities are of the order of 20,000 ft/sec the rear sheet of structures representative of space vehicle construction tends to fail as a result of rupturing and cracking with substantial rear sheet spallation and not as a result of perforation by individual fragments of the projectile and front sheet. Therefore, it may be concluded that any experimental evaluation of light space-vehicle structures must be based upon tests conducted upon realistic structures.

A number of firings must be made to bracket the structure's ballistic limit within a small velocity range. If the impact velocities are observed for firings which both exceed and are less than the ballistic limit, it is possible to determine the ballistic limit within an accuracy of 3 percent.

The effect of combined sheet thickness upon the penetration resistance of a double-sheet structure is shown in figure 1 where the ratio of combined sheet thickness to projectile diameter is plotted as a function of the ballistic limit with a constant value of 8 for the ratio of sheet spacing to projectile diameter. It can be seen that the curve presented in figure 1 is similar to curves obtained for impact into semi-infinite targets when the ratio of penetration to projectile diameter is plotted as a function of impact velocity. Thus, it is important to recall some results of thick target impact.

Charters and Summers in references 2 and 3 classified impact into thick targets into several categories which depend primarily on impact velocity. These categories are defined as, the undeformed projectile region, the transition region in which the projectile is broken, and the fluid impact region in which both projectile and target behave like fluids. It was observed that any penetration relations obtained in one region of impact were not applicable to other regions.

Impact in double-sheet targets also falls into several categories which again depend primarily on the velocity. These categories will be termed simply, the low-speed region, the transition region, and the high-speed region. The high-speed region, which is of primary interest, will be illustrated and discussed first.

Presented in figure 2 are a number of individual moving picture frames showing the results of a 1/8-inch-diameter pyrex glass sphere impacting a structure composed of two sheets of 2024-T3 aluminum alclad spaced at 1 inch with a combined sheet thickness of 1/8 inch. The impact velocity was 23,000 ft/sec and the movie was taken at 1.35×10^6 frames per second. Upon impact, both the projectile and the portion of target material removed from the front sheet are shattered into very fine fragments. The cloud of fragments forms a thin shell with few, if any, fragments in the shell interior. This is reasonable since, after impact, the hole in the front sheet grows radially and there is no material available to come in behind the shell front. The front of this shell is hemispherical in appearance as it approaches the second sheet and is traveling at about 60 percent of the impact velocity for this case. As the shell strikes the rear sheet a burst

of light is produced, and material splashes back to the rear of the front sheet with some of it passing out of the hole. It should be noted that the ambient pressure during the impact tests was sufficiently low that there was no deceleration of the hemispherical front. The luminosity results mainly from the small amount of air remaining in the chamber. Figure 3(a) presents an enlarged frame from the movie sequence shown in figure 2 and clearly shows the shell of finely shattered particles associated with impact at high speeds. Figure 3(b) presents a photograph of the rear sheet after impact. It can be observed that a large area of the sheet is more or less uniformly damaged. Consequently, the failure of the rear sheet from high-speed impact generally occurs in the form of small cracks radiating outward from the center of the damaged area, clearly indicating the rupturing effect of the effective particle pressure upon the sheet.

For the case of low-speed impact, target failure occurs in a manner quite different from that just discussed. Presented in figure 4(a) is an individual frame from a high-speed motion picture sequence taken during impact at 10,000 ft/sec. The projectile and the target material punched out of the front sheet forms a tight cluster of relatively large fragments as contrasted to the shell of fine fragments produced by impact at high velocity. Figure 4(b) presents a photograph of a typical rear sheet after impact at 10,000 ft/sec and shows the damage associated with impact within the low-speed impact region. It can be seen that although there is an over-all scattering of craters, the major damage is confined to a small central region, in contrast to the relatively large area for the high-speed case. The difference between the projectile break-up processes shown in figures 3(a) and 4(a) leads to the rear sheet damages shown in figures 3(b) and 4(b) and illustrates the high- and low-speed regions of impact in double-sheet targets.

The transition region contains those impacts in the velocity range where the projectile break-up process is changing from that of the low-speed case to that of the high-speed case. For different test conditions and, in particular, for different projectile materials, this velocity range may vary considerably. Consequently, the regions of impact should be defined in terms of fragmentation characteristics rather than by specific velocities. For the conditions of the investigations reported herein, the transition region occurs in the velocity range from 10,000 to 20,000 feet per second.

Relationships correlating the impact parameters in one region are not applicable to the others, just as was observed for impact into semi-infinite targets. At low speeds, it is apparent that combined sheet thickness varies with the first power of the velocity (see fig. 1) as does penetration in thick 2024-T3 aluminum targets as reported by Collins and Kinard in reference 4. However, as the impact velocity is increased, a transition region is reached where the character of impact begins to change from the low-speed type to the high-speed type as previously described. At velocities greater than about 20,000 ft/sec, required thickness appears to vary as the 2/3 power of the velocity. This is comparable to impact into semi-infinite targets as reported by Summers (ref. 3) who found that

penetration also varied with the 2/3 power of the velocity and was proportional to the kinetic energy of the projectile. Thus, it is thought that the penetration of double-sheet structures is also a function of the projectile kinetic energy at high speeds.

The effect of sheet spacing upon penetration resistance is illustrated in figure 5 where the ratio of sheet spacing to sphere diameter is plotted as a function of the target ballistic limit. At low speeds (velocities less than 10,000 ft/sec), spacing does not strongly affect the ballistic limit. This seems reasonable since it has been noted (see fig. 4(a)) that at low speeds the broken projectile and front sheet fragments remain in a tight cluster. The results obtained by Funkhouser in reference 5 indicate that spacings greater than 2 inches do little to improve the performance of a meteor bumper. At higher velocities, however, the transition region is reached and the spacing begins to become more effective. In the velocity range from 10,000 to roughly 20,000 ft/sec, projectile fragmentation is not complete and the optimum effectiveness of spacing is not realized. Within this region, the character of projectile and front sheet material break-up changes so rapidly with velocity that structural ballistic limit data cannot be obtained. However, at about 20,000 ft/sec, the high-speed region of impact is reached. Ballistic limit data within this region are still quite difficult to obtain because of the limited velocity capabilities of the guns now in use. In particular, it should be noted that the upper right square symbol shown in figure 5 is not an actual data point because the structure was not penetrated even at the highest speed attained (24,000 ft/sec). The arrow pointing toward the right that is associated with this symbol indicates that the ballistic limit of this target is greater than 24,000 ft/sec. In addition, an examination of the damage to this structure after impact at this velocity indicated that the ballistic limit was not lower than 26,000 ft/sec. This is not surprising since it can be seen in figure 3(a) that greater spacing allows the hemispherical shell to diverge over a greater area. Consequently, the dashed curve was drawn with the thought that the slope of this curve would give a conservative estimate of the effect of spacing within the high-speed region. Thus, the high-speed data shown in figure 5 show that spacing is much more effective at high speeds than at low speeds although an accurate evaluation of its effectiveness cannot be made at this time.

Effect of Front and Rear Sheet Weight Distribution

In connection with the above investigation, a limited test was conducted to determine the effect of front and rear sheet weight distribution upon penetration resistance. For this test, both the front and the rear sheets were 2024-T3 aluminum alclad and the ratios of combined sheet thickness to projectile diameter and of sheet spacing to projectile diameter were held constant at 1.0 and 8.0, respectively. From the data presented in the preceding section, it was apparent that structures expected to be resistant to meteoroid impact should be studied at the highest velocity attainable if meaningful results are desired.

Consequently, the structures described in this section were all impacted at a velocity of 20,000 ft/sec and all by 1/8-inch-diameter spheres.

The structures tested are tabulated in table I. It was observed that the first two structures shown have essentially the same ballistic limit. Thus, changing the front and rear sheet weight distribution from a 50-50 ratio to a 25-75 ratio results in no observable change in the performance of the structure. However, when the weight distribution was changed from a 50-50 ratio to a 75-25 ratio, a very marked decrease in performance was observed. It becomes obvious then that the front sheet of a structure serves primarily as a projectile break-up device and does not extract much energy from the system. Thus, the energy extracted by the front sheet of a structure as the sheet thickness is increased does not correspond to the loss of energy absorbing capabilities of the rear sheet as the thickness is decreased. Consequently, the optimum meteoroid-resistant double-sheet structure (with no intervening material) should probably consist of a meteor bumper just thick enough to completely fragment the projectile and a rear sheet containing the rest of the available weight. The necessary condition that the meteor bumper must completely shatter the projectile was investigated by impacting a structure weighing the same as the structures just described but with the weight divided between a 1-mil front sheet and a relatively thick rear sheet. It was observed that this structure was definitely inferior to the other structures tested. Consequently, there seems to be an optimum front to rear sheet weight distribution for double-sheet structures even at the impact velocities described herein. It seems reasonable to assume that at meteoric velocities, a very thin sheet will suffice to shatter the projectile so that the optimum weight distribution between sheets will be quite different from that observed at the relatively low velocities attainable in the laboratory. On the other hand, for impacts at meteoric speeds, the material splashed back from the rear sheet may destroy a substantial portion of such a front sheet.

Effect of Front Sheet Material

The investigations described previously were all restricted to aluminum targets. Additional tests were conducted to determine the effect of front sheet material upon penetration resistance. Front sheet materials were selected within a specific gravity range from 1.2 to 8.5 and the thickness of the sheets was selected so that the total mass per unit area remained constant throughout this test series. The rear sheet of all structures was 2024-T3 aluminum alclad and the ratio of sheet spacing to projectile diameter was held to a constant value of 8.0. Again all structures were impacted by 1/8-inch-diameter glass spheres and at a velocity of 20,000 ft/sec so that the results should be applicable to the high-speed region of impact. The structures tested in this program are also presented in table I. It was anticipated that the structures would simply be compared with one another to assess the relative performances. The result was, however, that all structures tested and presented in table I have essentially the same ballistic limit. Consequently, it may be concluded that, for a given mass per unit area of the meteor bumper, the bumper material is unimportant, at least within the limits of this investigation.

It can be seen that the difference in strength of the two brass sheets has no observable effect on the performance of the bumpers in providing protection.

A meteor bumper (not shown in table I) made of window glass was also tested simply to show the effect of brittleness. The glass was covered on the back side with masking tape but a small clear area was left for the projectile to strike. The bumper was completely shattered as the result of the strong shock waves produced. Without the masking tape, the entire 6-inch-square plate would have been pulverized. Therefore, if a brittle material is required for the outer surface of a space vehicle, perhaps as an ablative material for reentry, then a bonded, tough back-up structure would also be required. The protection provided for the second sheet by the glass bumper was consistent with its density just as noted for the bumpers of other materials.

Effect of Oblique Impact

In addition to the previously described tests conducted with the targets normal to the projectile trajectory, limited firings were made with the targets at oblique angles. It has been suggested many times that most of the meteoroid impacts will be on oblique surfaces and, therefore, the hazard would be materially reduced. Figure 6 presents individual movie frames of a 1/8-inch-diameter glass sphere striking a double-sheet aluminum target at an angle of 45° at 19,000 ft/sec. A witness sheet, used to assess the relative damage of the rear sheet, can be observed as the third sheet of this target and is not considered to be part of the structure under investigation. After impact, a complex spray pattern develops. Material is spalled off normal to the back of the front sheet and a cluster, similar to that described previously for the low-speed impact case, is formed which travels along the original trajectory of the pellet. In the case shown, the spall traveling normal to the front sheet strikes the rear sheet first and perforates it. A short time later, the cluster arrives at the rear sheet and also perforates it. Figure 7 presents a photograph of both sheets of the structure shown in figure 6 and clearly shows the damaged areas associated with the spray and cluster formations of oblique impact. There is a striking similarity between the rear sheet damage associated with the normal spray and the rear sheet damage produced by high-speed normal impact, as seen in figure 3(b). The damage produced by the normal portion of the oblique impact spray exhibits the same characteristics as that produced by normal impact in the high-speed impact region described in a previous section. In addition, when that portion of the damage produced by the oblique cluster is compared with the damage associated with normal impact in the low-speed impact region as seen in figure 4(b), it can be observed that there is again a close similarity. It can be concluded then, that for oblique impact within the velocity limits of this investigation, the spray traveling normal to the front sheet behaves in the same manner as the hemispherical shell of high-speed normal impact and that the oblique cluster behaves

like the low-speed normal impact cluster and produces the corresponding type of rear sheet damage. From this conclusion one can reason that if an oblique target is impacted at a velocity less than that of the case shown in figures 6 and 7, then the general spray pattern will tend to be more representative of low-speed impact and the cluster traveling along the line of the trajectory will produce the most significant rear sheet damage. This is illustrated in figure 8 which shows both sheets of a target after impact at the relatively low velocity of 10,000 ft/sec and at an angle of obliquity of 45°. It can be seen that the major portion of the rear sheet damage was produced by the oblique cluster, as expected, and that relatively little damage was caused by the normal spray. Thus, it may be stated that, as the impact velocity upon oblique targets is increased, rear sheet damage tends to be produced to a greater extent by the spray traveling normal to the front sheet and to a lesser extent by the cluster traveling along the line of the projectile trajectory. From this observation, it may be reasoned that for oblique impact at meteoric speeds, the spray pattern developed will be very similar to that of normal impact in the high-speed impact region and the rear sheet damage will be produced primarily, if not completely, from the spray normal to the front sheet. Note that the eccentricity of the hole in the front sheet is less for the higher impact velocity. This is in agreement with the data presented in reference 3.

With regard to the quantitative effects of obliquity on impact damage, the ballistic limit of the normal target was 9,500 ft/sec whereas the ballistic limit of the oblique target was 19,500 ft/sec. However, caution should be used in applying these results to estimate the effects of obliquity at meteoric speeds since the failure of the normal target occurred in the low-speed region and that of the oblique target in the transition region where both high- and low-speed effects were observed.

Front Sheet Hole Formation

Observations were made also of the formation of the hole in the front sheet for the case of normal impact. Figures 9 and 10 are photographs of sections of sheets impacted at low speeds (4,000 ft/sec) and high speeds (20,000 ft/sec), respectively. Shown in both figures are targets made of a soft, ductile aluminum alloy (1100-H14) and a strong, brittle aluminum alloy (2024-T3). From figure 9, it is apparent that for the low-speed impact case hole formation results from a punching or shearing action. The impact and exit surfaces of the targets are readily distinguished. Such is not the case, however, for impact at 20,000 ft/sec (see fig. 10). The sheets are perforated in a fraction of a microsecond during which the removed target material and projectile material are shattered into a multitude of tiny fragments forming the diverging shell described earlier. The hole in the sheet, however, continues to grow radially for many microseconds after impact (see fig. 2). Furthermore, this radial growth is symmetrical about the center of the sheet making it impossible to distinguish between the front and back surfaces of the sheets.

Measurements were made of the minimum hole diameters in the front sheets of the various targets. Plotted in figure 11 is the ratio of hole to projectile diameter as a function of the impact velocity for several values of sheet thickness to projectile diameter ratio. For a thickness to diameter ratio of 0.5, the data above 14,000 ft/sec are represented reasonably well by the equation given which was obtained from a log-log plot. It can be reasoned that since hole diameter varies as the square root of the impact velocity, then the mass of target material removed varies as the first power of velocity, that is, in proportion to the momentum of the projectile. It should be emphasized, however, that this result may very well be fortuitous since much of the data were obtained at velocities where the effects of transition from the low-speed to the high-speed type of impact are significant.

A limited amount of data were obtained for thickness to diameter ratios other than 0.5. These data were extrapolated to 20,000 ft/sec and a cross plot was made of hole to projectile diameter ratio as a function of thickness to diameter ratio as shown in figure 12. It can be seen that hole diameter varies linearly with thickness up to a value of nearly 0.5 for the thickness to diameter ratio. With further increase in sheet thickness, the rate of change in hole diameter decreases with increasing thickness and will eventually reach that value for a semi-infinite target.

CONCLUDING REMARKS

The present experimental investigation concerned with the impact resistance of simple double-walled structures of varying thickness and spacing has brought to light two significant results. First, it has been shown that the physical process of damage to a structure changes drastically with impact velocity. With increasing speed, shock damage plays an increasingly important part in causing failure and will undoubtedly be one of the most significant factors, if not the most significant, in causing structural failure at meteoric speeds. Consequently, if a structure is to be assessed for its resistance to meteoroid impact, then it most certainly must be tested at the very highest velocity attainable. Second, it is concluded that any evaluation of space vehicle structures must be based upon tests of realistic specimens because of the complex nature of the failure.

Ames Research Center
National Aeronautics and Space Administration
Moffett Field, Calif., June 29, 1962

REFERENCES

1. Nysmith, C. Robert, and Summers, James L.: Preliminary Investigation of Impact on Multiple-Sheet Structures and an Evaluation of the Meteoroid Hazard to Space Vehicles. NASA TN D-1039, 1961.

2. Charters, A. C., and Locke, G. S., Jr.: A Preliminary Investigation of High-Speed Impact: The Penetration of Small Spheres Into Thick Copper Targets. NACA RM A58B26, 1958.

3. Summers, James L.: Investigation of High-Speed Impact: Regions of Impact and Impact at Oblique Angles. NASA TN D-94, 1959.

4. Collins, Rufus D., Jr., and Kinard, William H.: The Dependency of Penetration on the Momentum Per Unit Area of the Impacting Projectile and the Resistance of Materials to Penetration. NASA TN D-238, 1960.

5. Funkhouser, John O.: A Preliminary Investigation of the Effect of Bumpers as a Means of Reducing Projectile Penetration. NASA TN D-802, 1961.

TABLE I.-DOUBLE SHEET STRUCTURES HAVING BALLISTIC LIMIT OF APPROXIMATELY 20,000 FT/SEC; SPACING = 1 INCH, d = 0.125 INCH

[All structures have same weight per unit area]

Front sheet		Rear sheet	
Material	Thickness, in.	Material	Thickness, in.
2024-T3	0.062	2024-T3	0.062
2024-T3	.031	2024-T3	.093
Hard brass	.010	2024-T3	.093
Soft brass	.010	2024-T3	.093
Acrylic	.075	2024-T3	.093

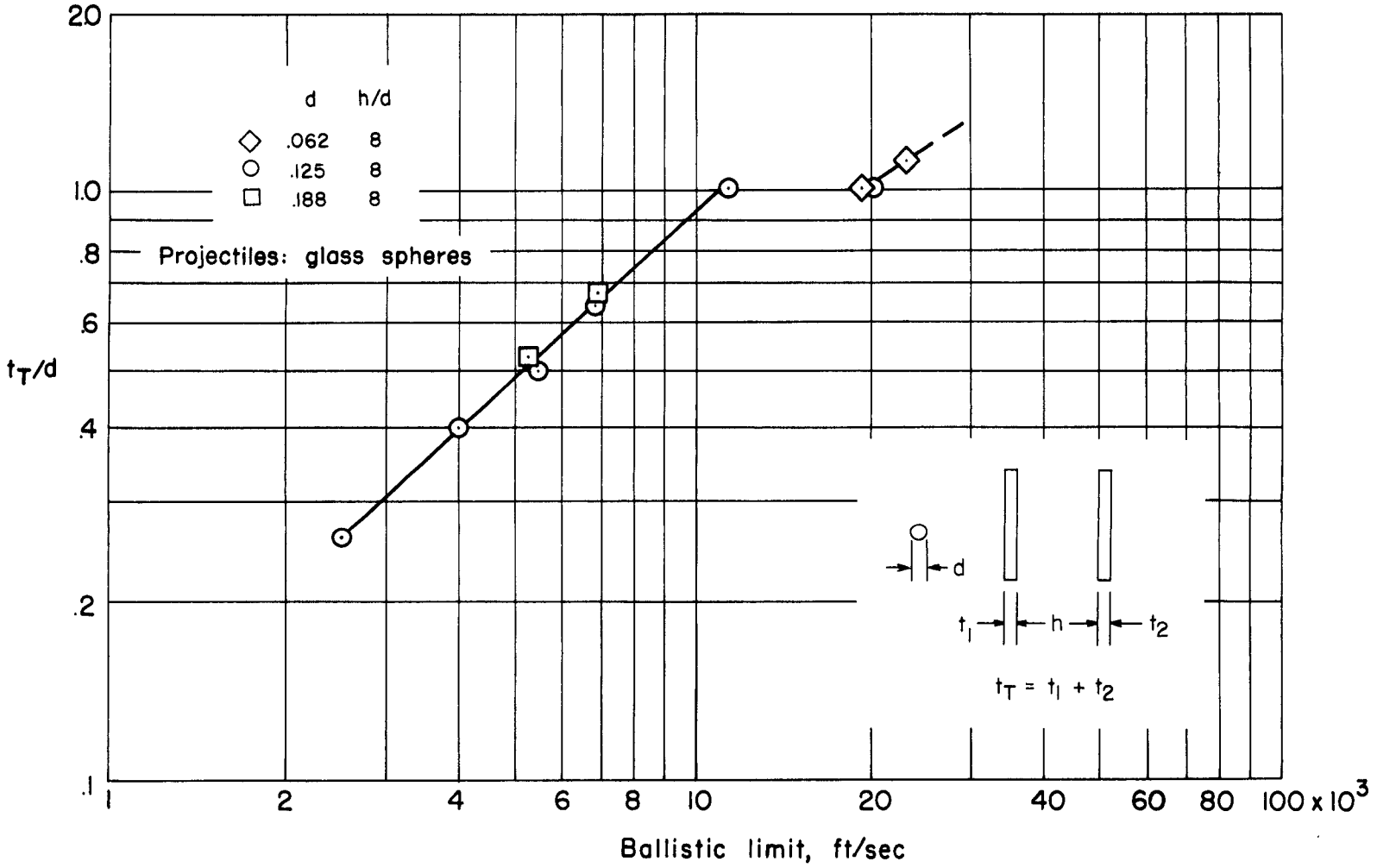

Figure 1.- Effect of thickness on ballistic limit of double-sheet structures.

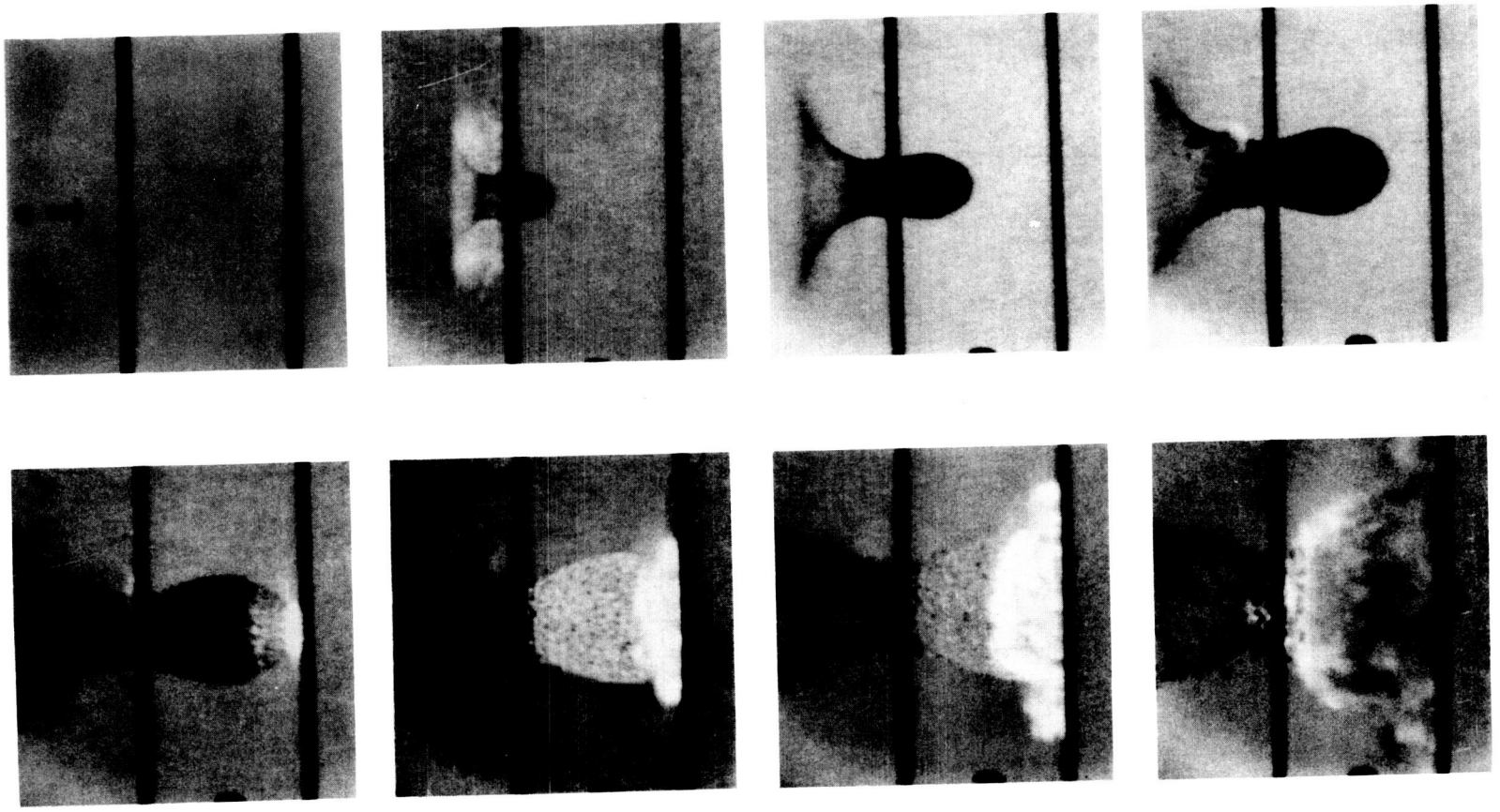

Figure 2.- Movie sequence of high-speed impact; V = 23,000 feet per second.

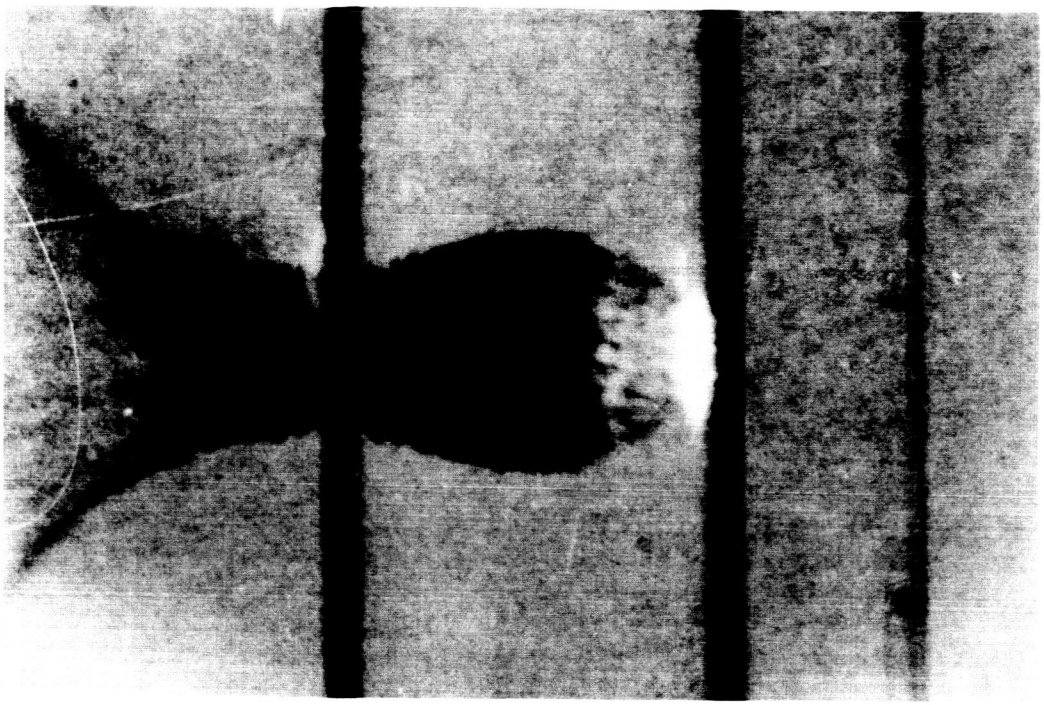

(a) Shell pattern.

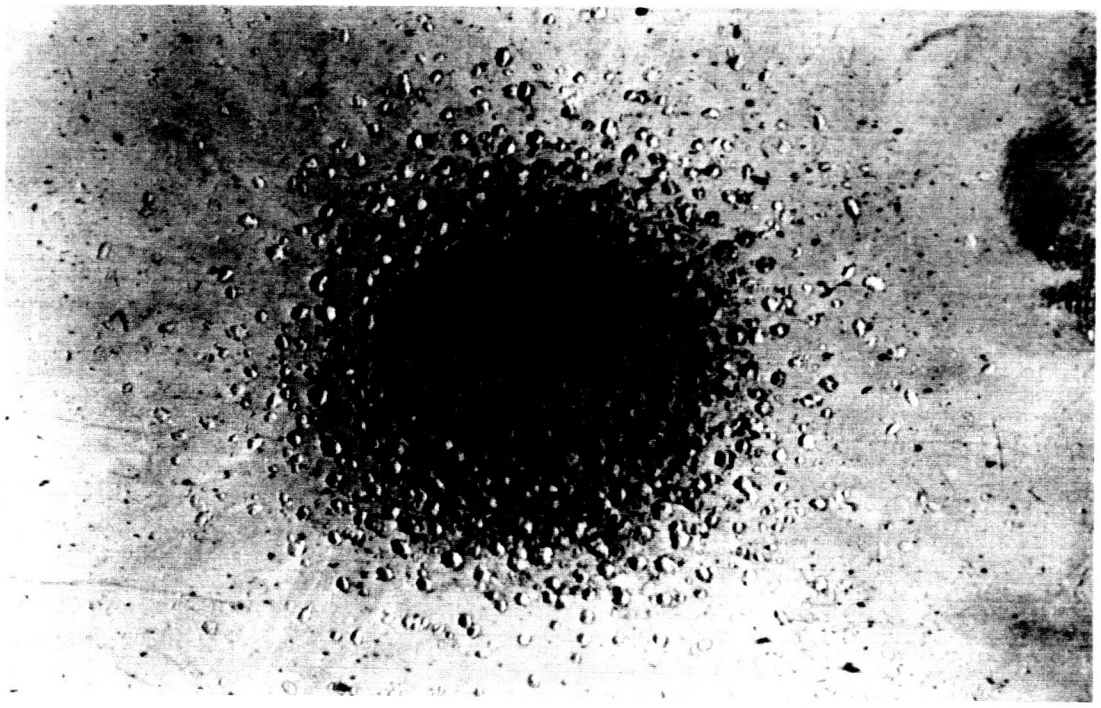

(b) Rear sheet damage.

A-27963.1

Figure 3.- Characteristic features of high-speed impact; V = 23,000 feet per second.

(a) Cluster pattern. A-27877-5

(b) Rear sheet damage. A-27964.1

Figure 4.- Characteristic features of high-speed impact; V = 10,000 feet per second.

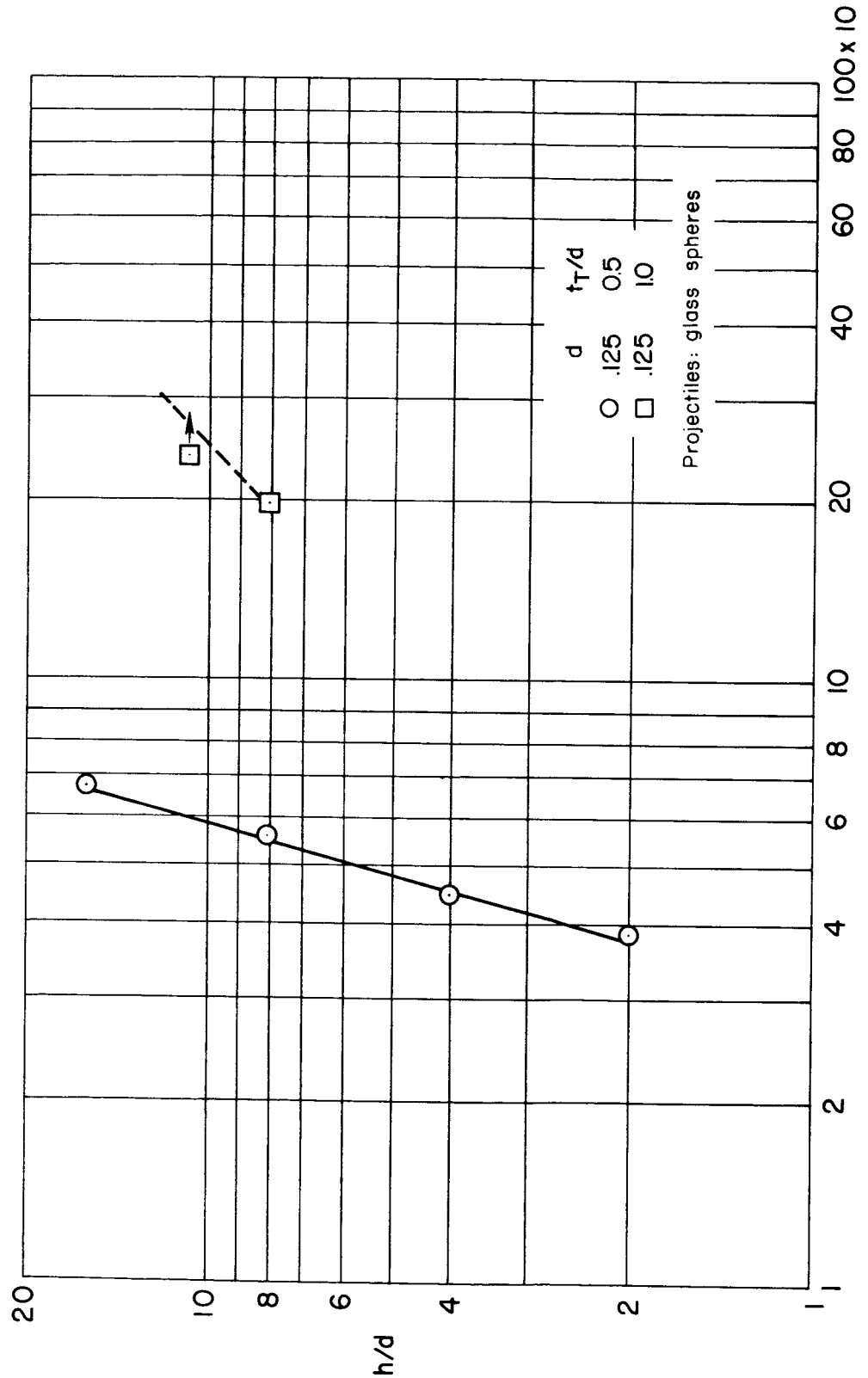

Figure 5.- Effect of spacing on ballistic limit of double-sheet structures.

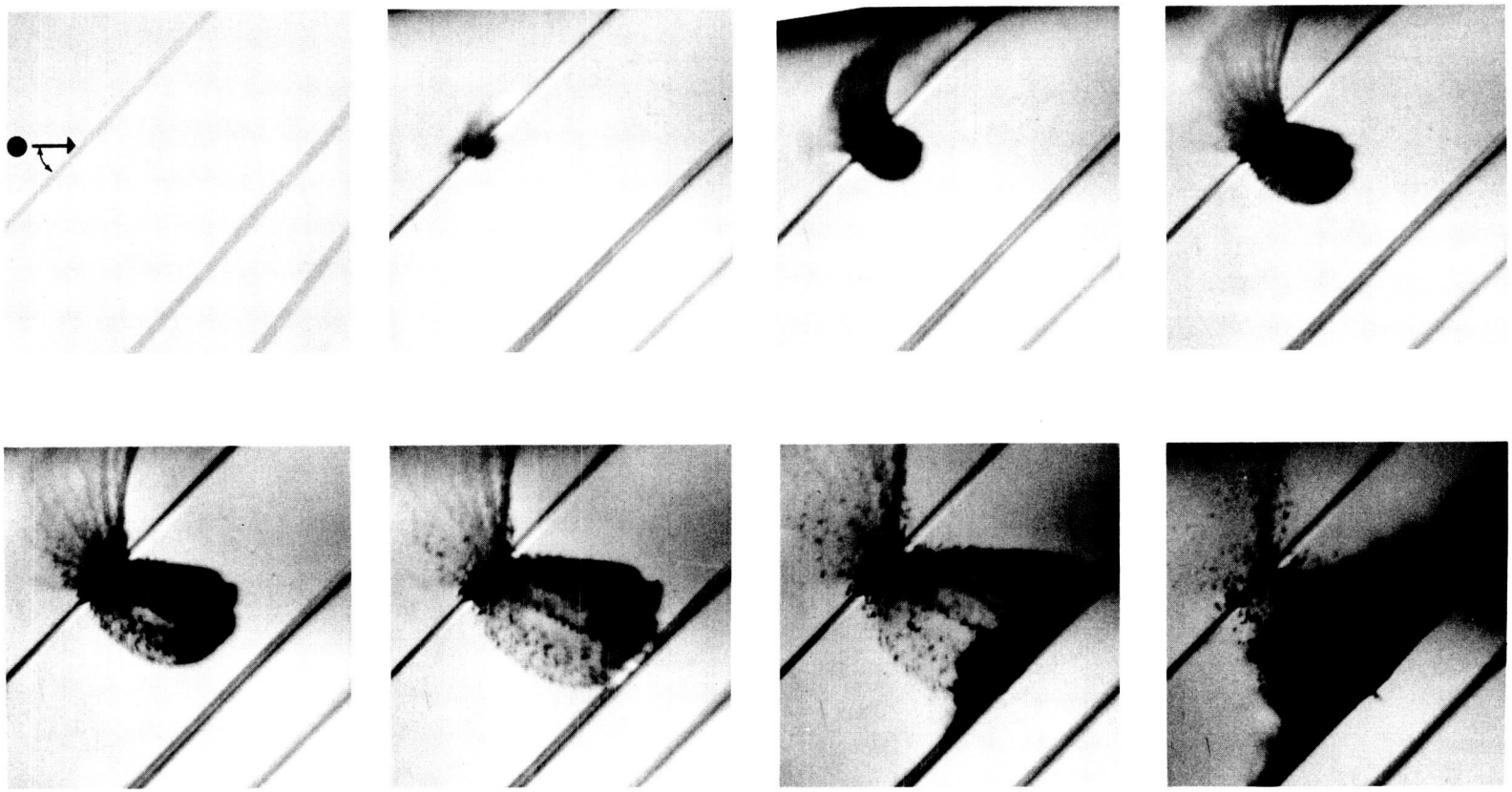

Figure 6.- Movie sequence of 45° oblique impact; V = 19,000 feet per second.

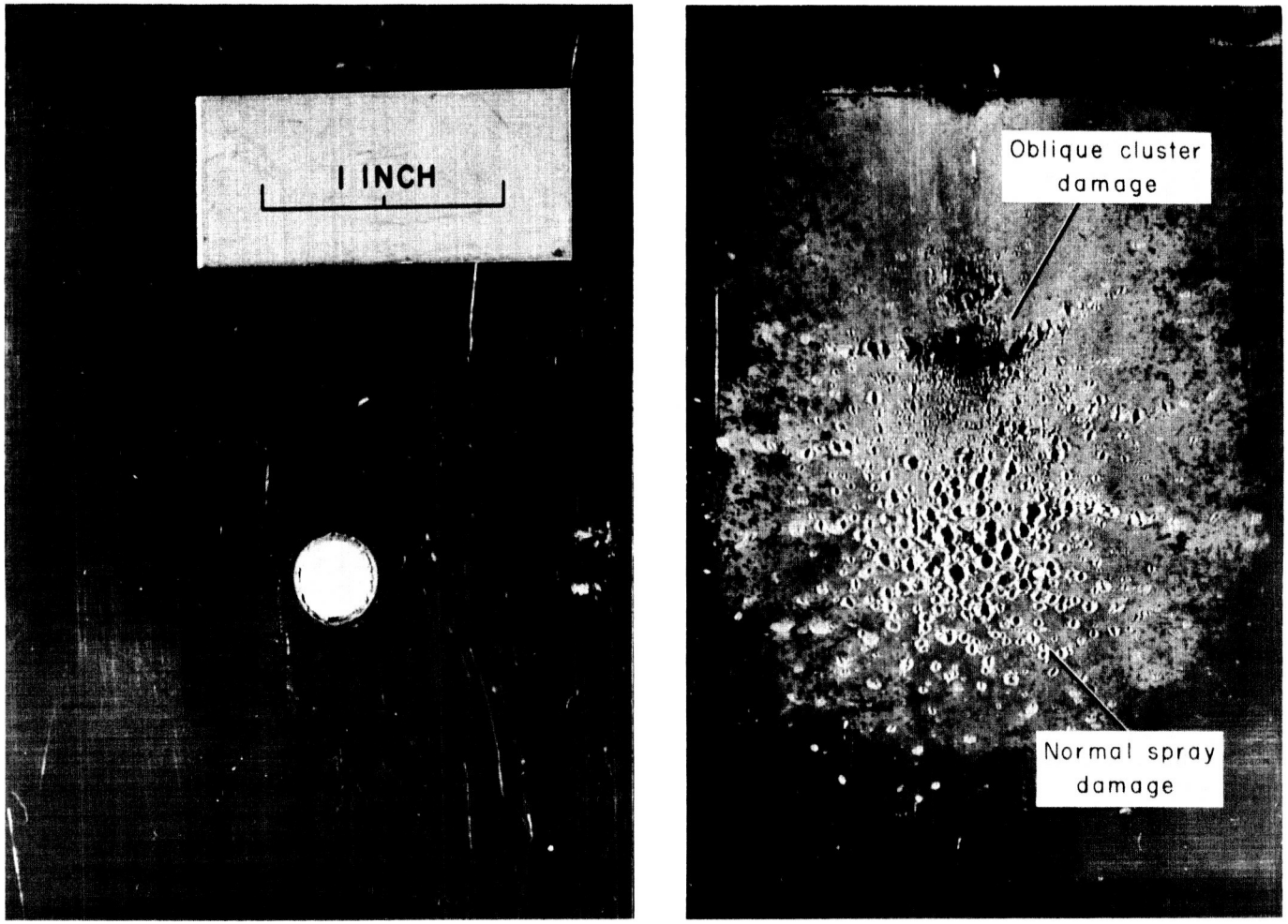

(a) Front sheet.

(b) Rear sheet.

A-28643.1

Figure 7.- Front and rear sheets of target after 45° oblique impact; V = 19,000 feet per second.

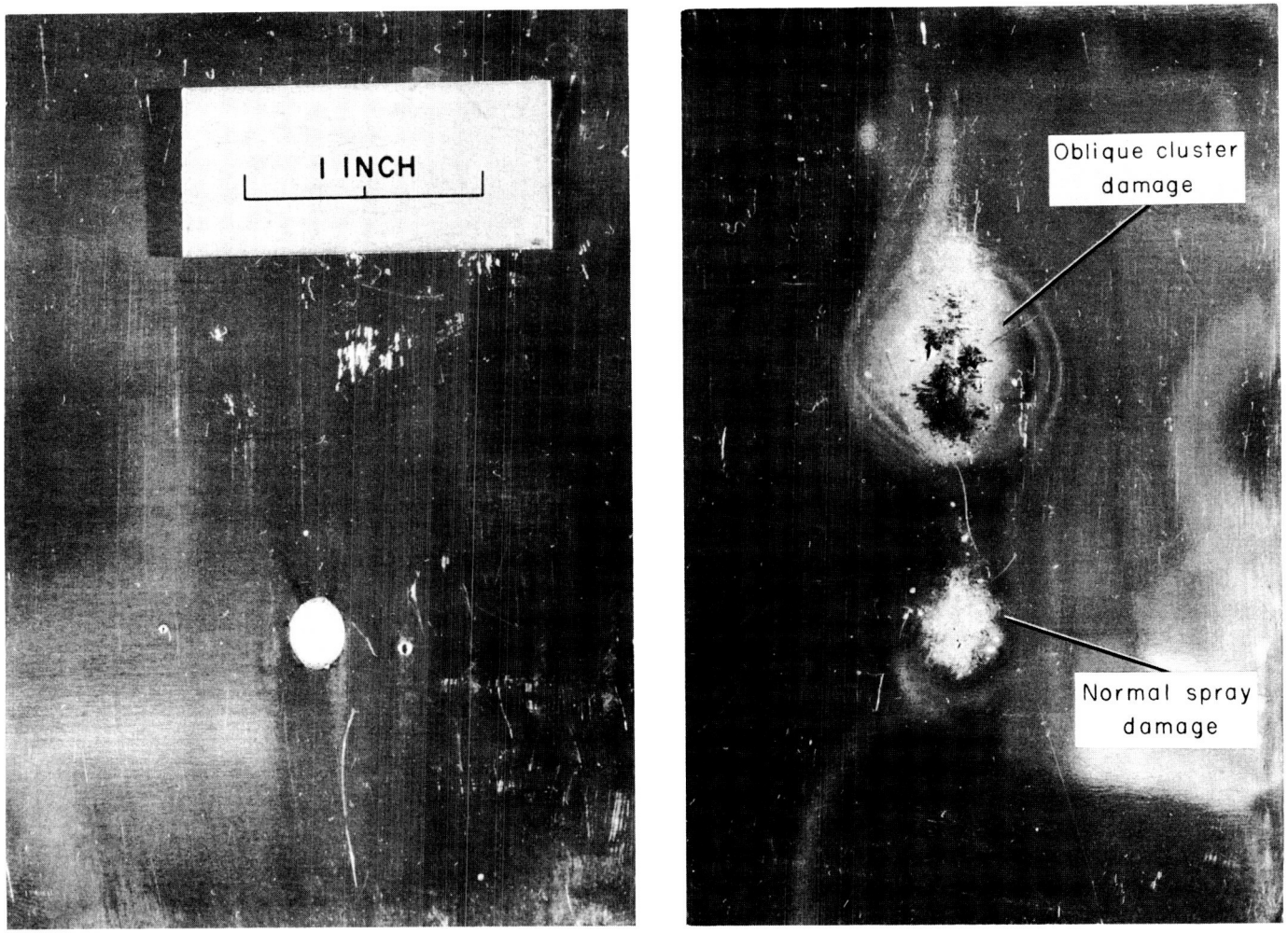

(a) Front sheet.

(b) Rear sheet.

A-28645.1

Figure 8.- Front and rear sheets of target after 45° oblique impact; V = 10,000 feet per second.

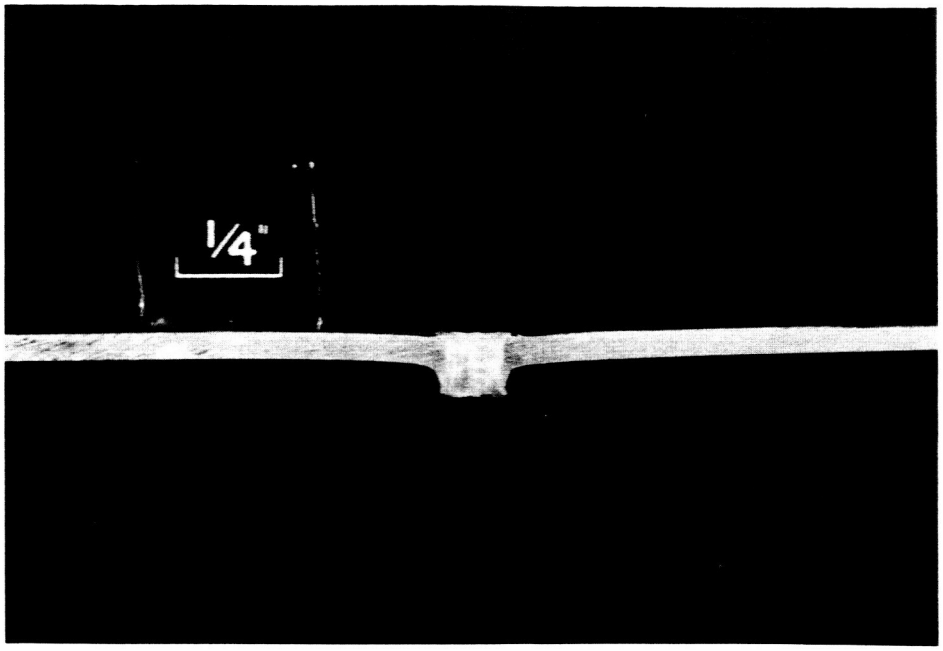

(a) 1100-H14 alloy. A-29398

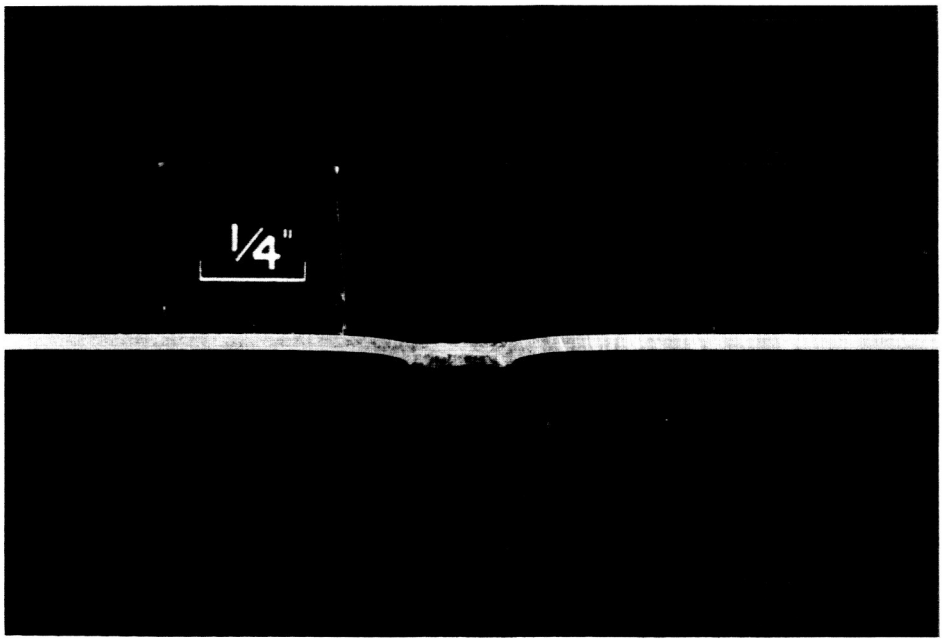

(b) 2024-T3 alloy. A-29399

Figure 9.- Section views of targets impacted at low speed; V = 4,000 feet per second.

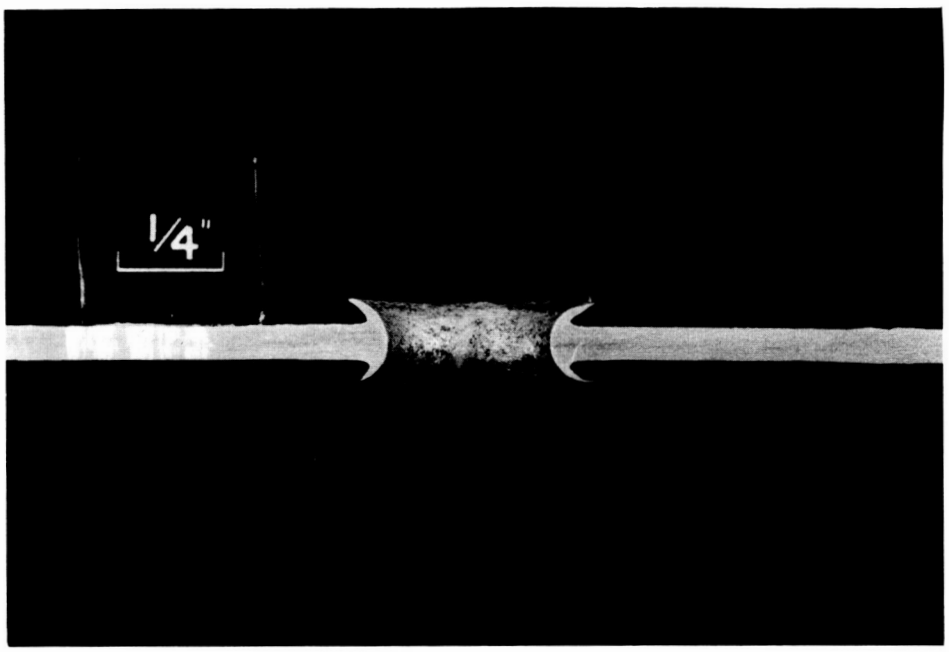

(a) 1100-H14 alloy. A-29400

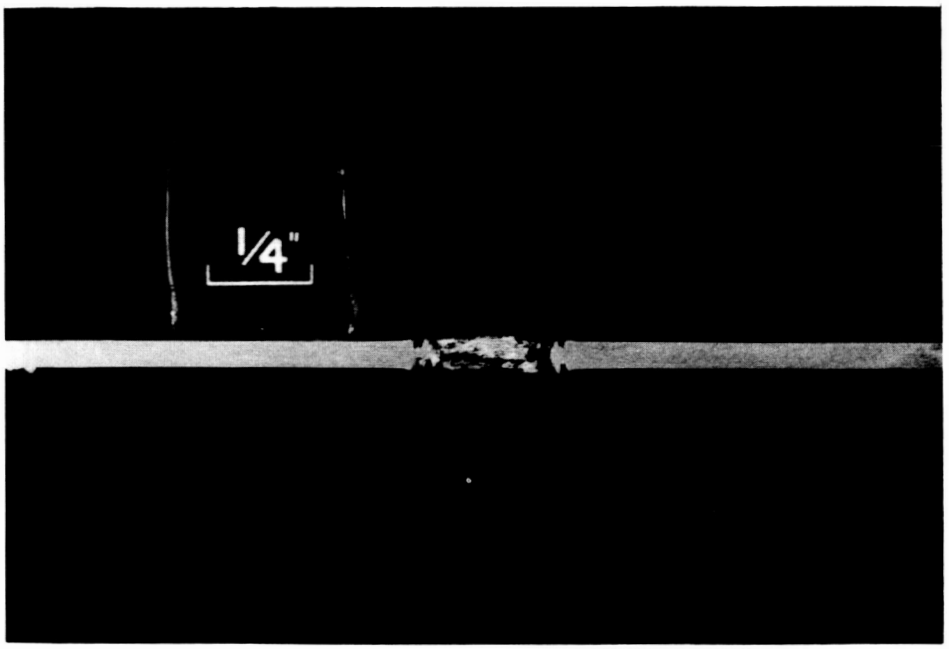

(b) 2024-T3 alloy. A-29401

Figure 10.- Section views of targets impacted at high speed; V = 20,000 feet per second.

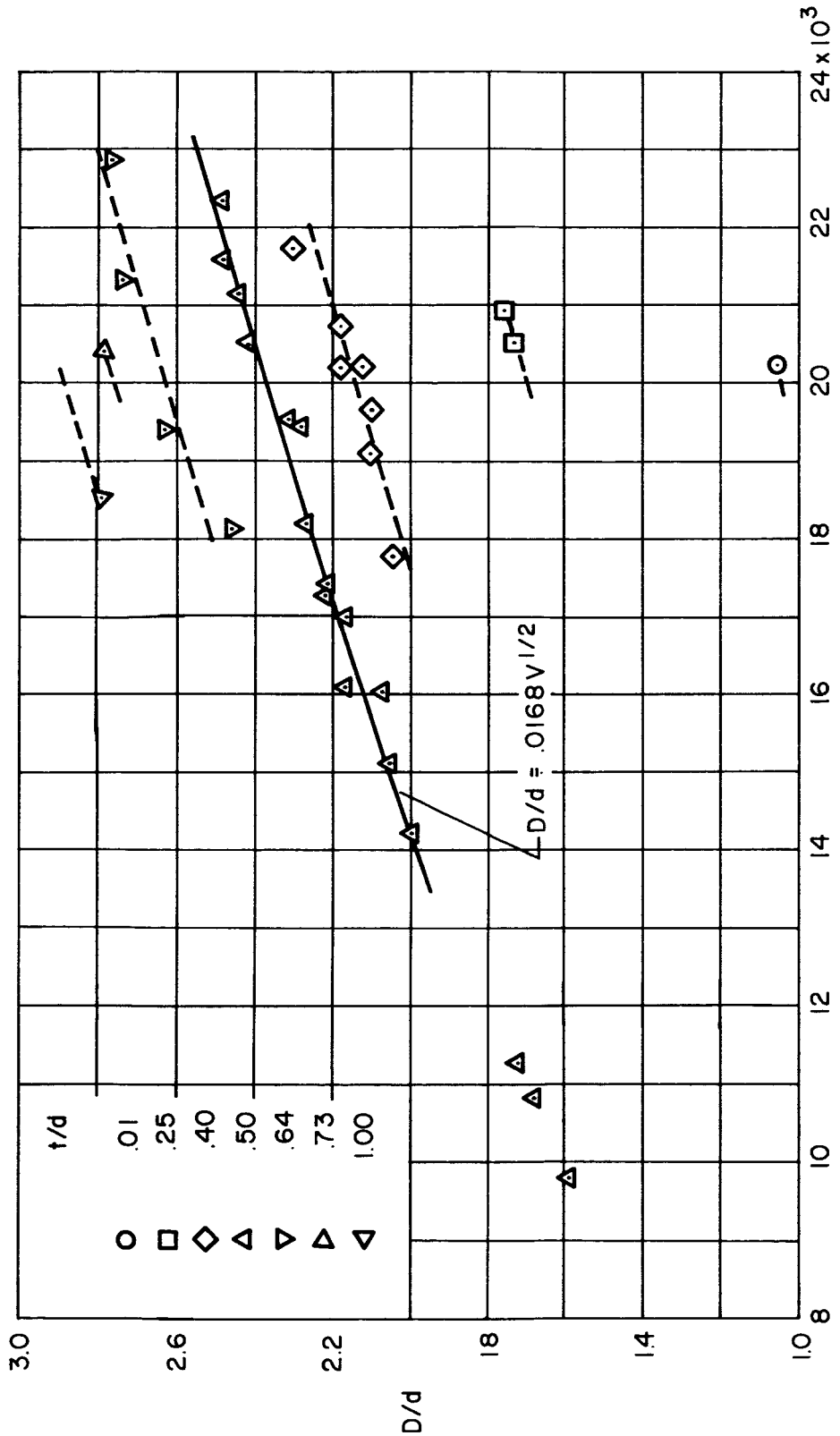

Figure 11.- Variation of front-sheet hole-diameter ratio with impact velocity.

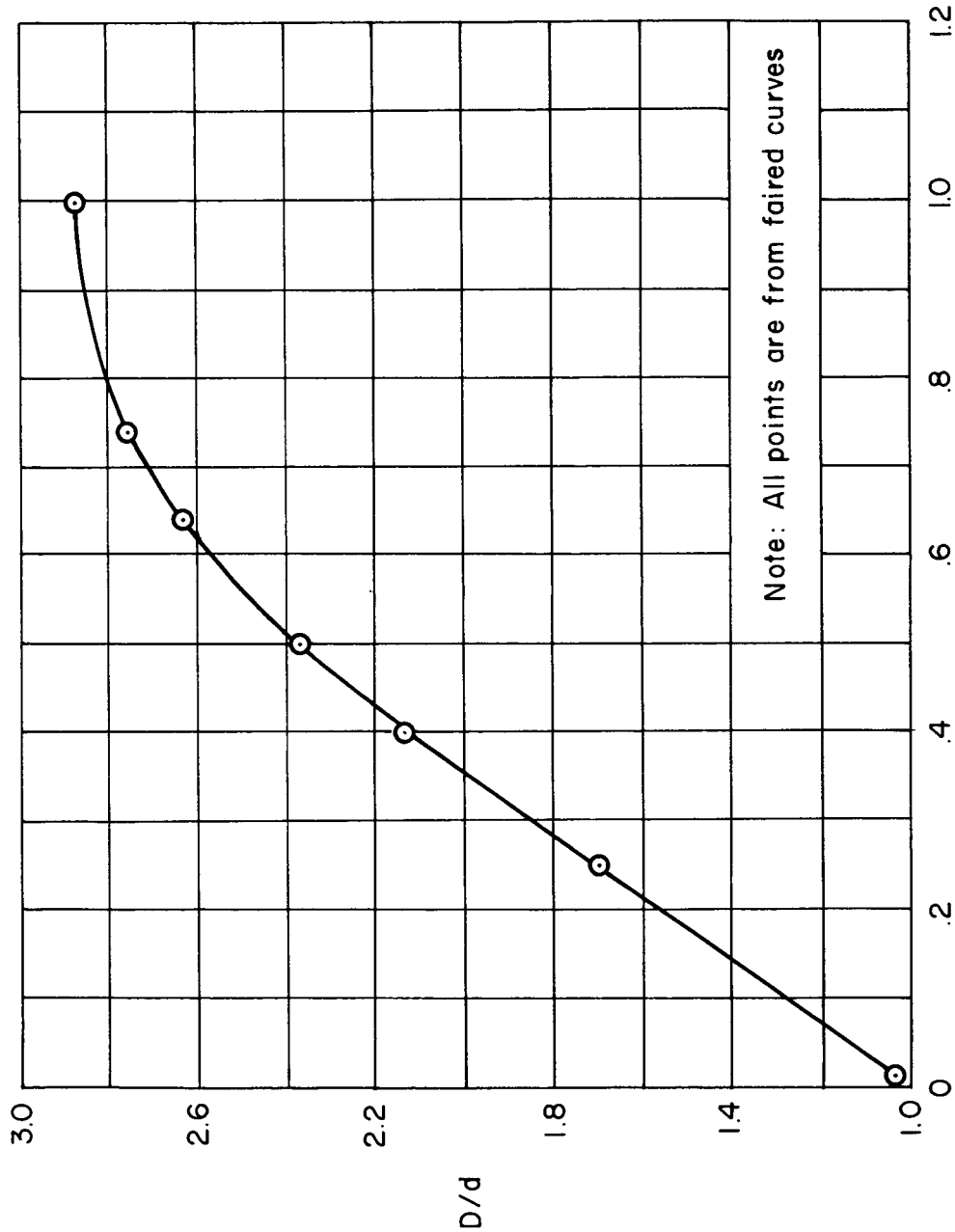

Figure 12.- Variation of front sheet hole-diameter ratio with thickness ratio for an impact velocity of 20,000 feet per second.